

Research Article

Kun Zhang, Jun Peng*, Xin Wang, Zhenxue Jiang, Yan Song, Lin Jiang, Shu Jiang, Zixin Xue, Ming Wen, Xiaohui Li, Xiaoxue Liu, Yizhou Huang, Pengfei Wang, Chang'an Shan, Tianlin Liu, and Xuelian Xie

Effect of organic maturity on shale gas genesis and pores development: A case study on marine shale in the upper Yangtze region, South China

<https://doi.org/10.1515/geo-2020-0216>

received July 12, 2019; accepted November 16, 2020

Abstract: The marine shale in southern China has undergone complex tectonic evolution with a high thermal evolution degree. Excessive thermal evolution brings certain

* **Corresponding author: Jun Peng**, School of Geoscience and Technology, Southwest Petroleum University, Chengdu, 610500, China, e-mail: pengjun@swpu.edu.cn

Kun Zhang: School of Geoscience and Technology, Southwest Petroleum University, Chengdu, 610500, China; State Key Laboratory of Oil and Gas Reservoir Geology and Exploitation, Southwest Petroleum University, Chengdu 610500, China; Key Laboratory of Tectonics and Petroleum Resources (China University of Geosciences), Ministry of Education, Wuhan 430074, China

Xin Wang, Zhenxue Jiang, Zixin Xue, Ming Wen, Xiaohui Li, Xiaoxue Liu: State Key Laboratory of Petroleum Resources and Prospecting, China University of Petroleum, Beijing 102249, China; Unconventional Natural Gas Institute, China University of Petroleum, Beijing 102249, China

Yan Song: State Key Laboratory of Petroleum Resources and Prospecting, China University of Petroleum, Beijing 102249, China; Unconventional Natural Gas Institute, China University of Petroleum, Beijing 102249, China; Research Institute of Petroleum Exploration and Development, Beijing 100083, China

Lin Jiang: Research Institute of Petroleum Exploration and Development, Beijing 100083, China

Shu Jiang: Key Laboratory of Tectonics and Petroleum Resources of Ministry of Education, Faculty of Earth Resources, China University of Geosciences, Wuhan 430074, China; Research Institute of Unconventional Oil & Gas and Renewable Energy, China University of Petroleum (East China), Qingdao 266580, China; Energy and Geoscience Institute, University of Utah, Salt Lake City, Utah 84108, United States of America

Yizhou Huang: Organic Geochemistry Unit, School of Chemistry, University of Bristol, Cantock's Close, Bristol BS8 1TS, UK

Pengfei Wang: Geoscience Documentation Center, China Geological Survey, Beijing 100083, China

Chang'an Shan: School of Earth Sciences and Engineering, Xi'an Shiyou University, Xi'an 710065, China

Tianlin Liu: State Key Laboratory of Petroleum Resources and Prospecting, China University of Petroleum, Beijing 102249, China

risks to shale gas exploration and development. With the advancement of experimental methods, the evolution process of shale reservoirs can be better understood from the micro-nanoscale. This work takes the Ordovician-Silurian Wufeng and the first member of Longmaxi Formation in the Sichuan Basin and Lower Cambrian Niutitang Formation in Outer Margin of the Sichuan Basin to study the impact of maturity upon the genesis of shale gas and development features of the reservoir. A series of geochemical research methods, including TOC, gas component and gas isotope, were adopted to study the impact of different thermal evolution stages of organic matter upon the genesis of shale gas. The nanoscale micro-imaging technique, such as FIB-SEM and FIB-HIM, was used to analyze the development of OM-hosted pores. As shown from the results, when $R_o = 1.2\text{--}3.5\%$, the marine shale gas is dominated by methane and other hydrocarbon gases, since the mixture of cracking gas from liquid hydrocarbons and kerogen-cracking gas cause the carbon isotope reversal. Besides, the pyrobitumen pores characterized by the strong connectivity and storage capacity were primarily developed. When $R_o > 3.5\%$, the organic matter is at the graphitization stage. The shale gas is mainly composed of nitrogen at this stage. The nitrogen is originated from the atmosphere and the thermal evolution process, and the OM-hosted pores (pyrobitumen and kerogen pores) characterized by the bad connectivity and storage capacity are developed. Finally, the main component of shale gas, the genesis of shale gas and the pattern of OM-hosted pores under different thermal evolution stages of organic matter are summarized, which provide technical support for the exploration and development of shale gas.

Keywords: organic matter pores, carbon isotope reversal, source of nitrogen, kerogen-cracking gas, shale gas

Xuelian Xie: Guangzhou Marine Geological survey, Guangzhou 510760, China

1 Introduction

After the breakthrough of shale gas in the United States, the application and promotion of horizontal well hydraulic fracturing, micro-seismic monitoring, multi-well industrialized exploitation and other technologies have set off a “shale gas revolution” in the world, and shale gas is becoming an important domain for oil and gas exploration to be replaced [1–4]. China is rich in shale gas resources and began the exploration and development of shale gas after the United States and Canada [5,6]. In 2010, China National Petroleum Corporation (CNPC) made a breakthrough in the industrialization of shale gas by drilling Wei-201 well, the first shale gas evaluation well. Subsequently, Weiyuan, Changning, Zhaotong, Fushun-Yongchuan, Jiaoshiba, Dingshan and other shale gas fields were built successively, realizing large-scale development [7,8]. Despite there are a series of achievements made in shale gas exploration in China, the content of shale gas in different plays and layers varies greatly, with high-yielding wells, low-yielding wells and no-yielding wells appearing. Therefore, further study is still needed on the mechanism of shale gas enrichment. At present, the sedimentary environment [9–11], pore throat characteristics [12–14], the heterogeneity [15,16], the structural style of shale gas reservoir [17–19], the effect of rock anisotropy on gas permeability [20–22] and other issues have been extensively studied by the previous researchers [23–25]. Upper Ordovician-Lower Silurian shale and Lower Cambrian shale, in southern China, have good gas-bearing potential, rendering them the preferred targets for shale gas exploration. However, the two series of marine shale formations have undergone multiple stages of complex structural and thermal evolution with a high risk of exploration and development. Therefore, it is the prominent problem to study the impact of maturity upon the genesis of shale gas and development features of organic pores.

A series of studies have been conducted on the relationship between maturity and shale gas enrichment. Liang [26] thought that after the study of the lower Cambrian Qiongzhusi Formation shale in the north of Yunnan and Guizhou province in the southern Sichuan Basin, the content of TOC, kerogen type, clay mineral and maturity are the main controlling factors of microscopic pore structure, the influence of maturity is the most obvious, and the specific surface area and pore volume of shale decrease sharply with the increase of maturity. Wang [27] studied the Niutitang shale of the lower Cambrian in the upper Yangtze region and supposed that the high degree of thermal evolution resulted in the undeveloped pores of organic matter in the Niutitang Formation shale in the

study area, and the development of micro-nanopores with intergranular pores and intragranular pores is the main types. Pore evolution of organic matter and hydrocarbon generation evolution is not completely consistent in time. During the period of mass development of shale organic matter pores, the formation was not uplifted in time, which led to the further enhancement of the thermal evolution of the reservoir, the number of OM-hosted pores decreased sharply, and shale gas lost the effective storage space of organic matter pores after it was generated. Gao [28] studied the Wufeng Formation–Longmaxi Formation shale in southeast Chongqing and believed that the organic pores were mainly “spongy” pores densely distributed in the organic matter. When the R_o was between 1.56 and 3.5%, macropores and mesopores were the main ones, macropores decreased and mesopores and micropores increased when $R_o > 3.5\%$.

China’s shale gas companies have drilled a series of shale gas wells in the lower Cambrian and upper Ordovician-lower Silurian systems of the Sichuan basin, but the output varies widely. Exploration practice shows that maturity is the main controlling factor of shale gas enrichment, because of the large scope of marine sediments, Shale has strong homogeneity in the same block. The Jiaoshiba block in the southeastern part of the Sichuan Basin has achieved large-scale industrial development. The Jiaoye-1 well is the representative well of the Jiaoshiba block. However, the Youyang block located at southeast Chongqing, on the outer margin of the Sichuan Basin, does not have good commercial shale gas flow. The Youye-1 well is the representative well of the Youyang block, as shown in Figure 1. This article selects two representative wells, setting up a corresponding shale gas accumulation pattern through a series of experiments research. Through a series of experiments on the upper Ordovician Wufeng Formation, the first section of the strata of the lower Silurian Longmaxi Formation and the lower Cambrian Niutitang Formation, the effects of organic matter maturity on the shale gas genesis and the development of the organic pore, a corresponding shale gas accumulation model was established.

2 Geological Setting

2.1 Sedimentary and stratum characteristics

Large-scale transgression occurred in the Yangtze area in the early Cambrian, and the study area was in the sedimentary environment of the deep-water continental

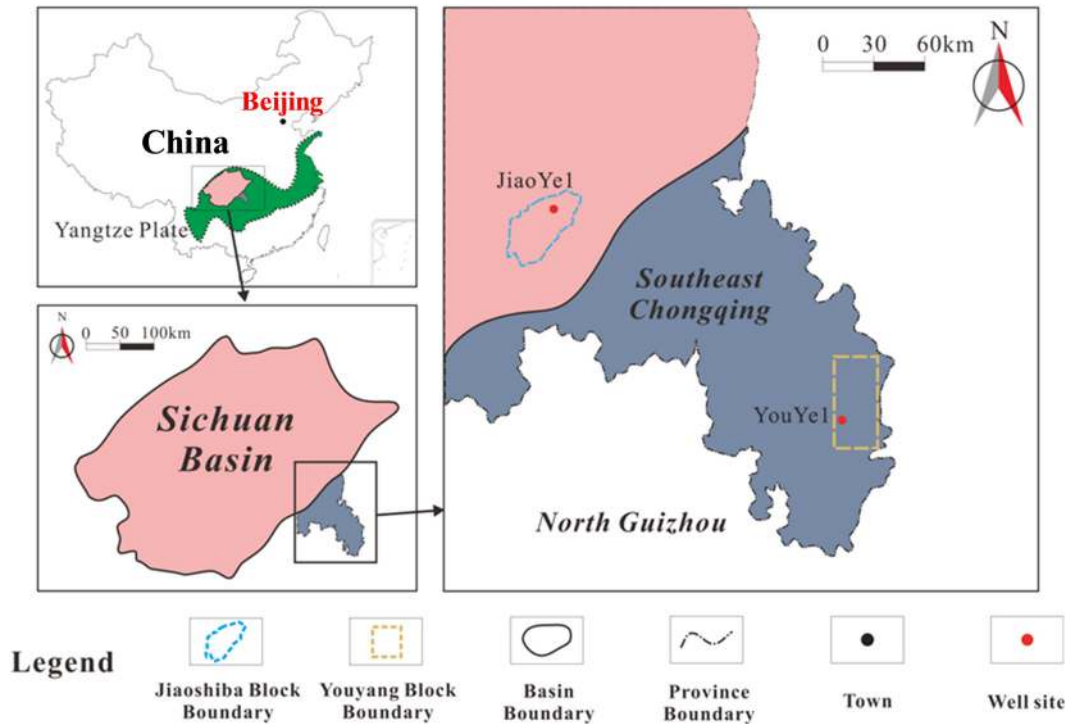


Figure 1: The distribution diagram of the Jiaoye-1 well in the Jiaoshiba block, southeast Sichuan basin, and Youye-1 well in the Youyang block, southeast Chongqing, outer margin of Sichuan basin.

shelf. The high biological productivity, anoxic and reducing environment and relatively developed hydrothermal activity were conducive to the accumulation of organic matter in shale, forming the Niutitang Formation shale with high-organic matter content, wide distribution range and large thickness [29–31]. As shown in Figure 2a, the upper strata (3,737–3,795 m) of Niutitang Formation in Youye-1 well are dominated by dark gray argillaceous limestone, the middle strata (3,795–3,845 m) are the black organic-rich shale and the lower strata (3,845–3,861 m) are dark gray siliceous shale.

During the late Ordovician and the early Silurian, due to the convergent collision between the Yangtze plate and Cathaysia plate, the upper Yangtze region is in the deep-water shelf environment surrounded by ancient land, which led to strong sealing ability and appears stratified phenomenon of the water body. It has deposited the Ordovician-Silurian Wufeng and Longmaxi Formation shale with high-organic matter content, large thickness and wide distribution [32–34]. As shown in Figure 2b, Wufeng Formation and the lower part of the first section of Longmaxi Formation in Jiaoye-1 well are black organic-rich shale, and the upper part of the first section of Longmaxi Formation is dark gray silty shale. The underlying strata of Wufeng Formation are gray nodular limestone of Lin Xiang formation of the upper Ordovician, and the

overlying strata of the first section of Longmaxi Formation are gray argillaceous siltstone of the second section of Longmaxi Formation.

2.2 Tectonic characteristics

The research area is located in the upper Yangtze region. According to previous studies [35–37], the early Cambrian of the Yangtze plate and the Cathaysia plate in southern China was still in a state of separation. Because of the massive transgression, almost throughout the Yangtze plate deposited a set of Organic-rich shale. Later, as the water body becomes shallow gradually, the lithology evolved from fine shale and silty shale to coarse-grained clastic rocks such as siltstone and sandstone. In Ordovician, affected by the collision between the Cathaysia plate and Yangtze plate, the water body continued to become shallower, and the clastic sedimentary system was transformed into a carbonate sedimentary system. In the late Ordovician and early Silurian, due to the melting of glaciers, large-scale transgression occurred again, which turned into a clastic rock sedimentary system again and a set of organic shale was deposited in the deep-water shelf area surrounded by the ancient land with strong sealing.

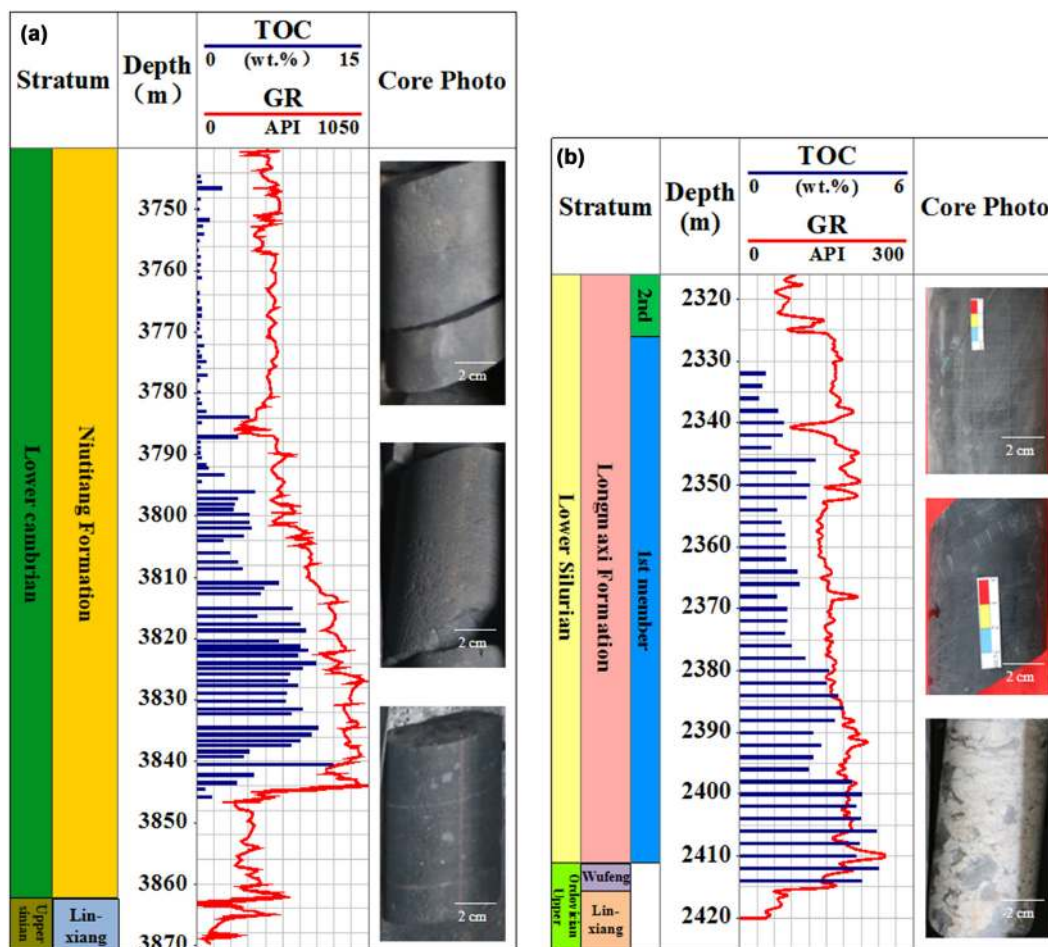


Figure 2: The comprehensive stratigraphic histogram and core photographs. (a) The lower Cambrian Niutitang Formation of Youye-1 well, (b) the section of the upper Ordovician Wufeng Formation and the first section of the lower Silurian Longmaxi Formation of Jiaoye-1 well. See Figure 1 for the well locations.

3 Samples and methods

3.1 Carbon and nitrogen isotopic analysis and gas component differences

The shale gas samples were taken from the Wufeng Formation–Longmaxi Formation of Jiaoye-1 well (Number: 1–8) and the Niutitang Formation of Youye-1 well (Number: 9–16). Eight gas samples were taken from each well, 16 samples in total. All 16 samples were analyzed with the Matrix-MG gas analyzer for composition: the 8 gas samples from Jiaoye-1 well were analyzed with the Trace GCULTRA-MAT 253 IRMS gas isotope analyzer for carbon isotope composition and the 8 gas samples from Youye-1 well were analyzed with the same for nitrogen isotope analysis. Some data are quoted from previous studies [38–40].

3.2 TOC analysis

A total of 42 rock core samples were sampled at the Wufeng Formation–Longmaxi Formation section of the Jiaoye-1 well with an interval of 2 m. A total of 86 rock core samples were sampled at Niutitang Formation of the Youye-1 well with an interval of about 0.5–3 m. The TOC was analyzed with the OG-2000V carbon and sulfur analyzer.

3.3 FIB-SEM observation

Focused Ion Beam Scanning Electron Microscopy (FIB-SEM) is a method to focus a beam of ions on and scanning over the samples. The atomic bombardment on the surfaces of the samples by the ion beam will sputter the atoms. It provides a neotechnology for the research of the micro-

nanopores. In this paper, two organic-rich shale samples with relatively high TOC taken at 3,811 m of the Niutitang Formation in the Youye-1 well and at 2,406 m of the Longmaxi Formation in the Jiaoye1 well were given FIB-SEM analysis. The instrument used was an FEI-HELIOS-NanoLab 650 manufactured by the US FEI Company. Before observation, the rock samples received the surface preparation with argon ion polishing and conductive layer spraying for clearer images. As observed with the backscattering function, the appearance of the organic matter was black with the lowest brightness, the appearance of the pyrite was white with the highest brightness, and the appearance of the matrix minerals such as quartz and calcite was light gray. The pores were black notably. And the secondary electrons generated from the sample surface by ion beam bombardment highlighted the periphery of the pores while other nonpore areas were not highlighted.

3.4 FIB-HIM observation

Focused ion beam-helium ion microscopy (FIB-HIM) is a method that integrates the imaging function of the high-resolution helium ion microscope with the cutting function of the focused ion beam and the helium ion beam. The resolution of FBI-HIM is as high as the sub-nanometer scale. The imaging with helium ion beam gives the 2D images certain 3D features, providing an easier way to observe the 3D shape of the pores and qualitatively determine the connectivity and development of the pores on the samples. Unlike the FIB-SEM, the appearance of the organic matter is gray under the bombardment of helium ions, and the matrix minerals such as quartz are black. The organic pores still in black can be easily identified from the organic matter. In this paper, the organic-rich shale samples were taken at 3,813 m of the Niutitang Formation in the Youye-1 well and at 2,404 m of the Longmaxi Formation in the Jiaoye-1 well were given FIB-HIM to further determine the connectivity and development of shale pores. The instrument used was a NanoFab-ORION Helium ion microscope manufactured by Carl Zeiss, Germany.

4 Results and discussion

4.1 Features of gas components

It can be seen from the gas composition analysis that the main component of the shale gas from the Ordovician-

Silurian Wufeng and Longmaxi Formation shale section of the Jiaoye-1 well was CH_4 with an average volume of 98.31% (Figure 3a). The main component of the shale gas from the Niutitang Formation of the Youye-1 well was N_2 with an average volume of 95.92%, and its average CH_4 content was only 1.40% (Figure 3b).

4.2 Features of organic pores development

4.2.1 Classification of OM-hosted pores

The organic matter in the shale can be divided into kerogen and pyrobitumen. Kerogen is formed from the original sedimentary organic matter undergoing the diagenetic stage. The pyrobitumen came from the process that the liquid hydrocarbon, formed in kerogen hydrocarbon generation, was filled into the mineral matrix pores, but not discharged from the organic-rich shale and underwent bituminization at the high-over mature stage with the secondary cracking gas generation.

The kerogen and pyrobitumen in the shale can be distinguished under the microscope based on their petrological features. The kerogen is mostly distributed in strips with inorganic mineral assemblage, which is due to the *in situ* sedimentation of organic matter during the sedimentary process. The irregular distribution of pyrobitumen is formed in the above-mentioned formation process and its patterns dependent on the patterns of the intragranular pores and intergranular pores of the shale. Its boundary with the minerals is clear without inorganic mineral assemblage.

The OM-hosted pores are the secondary pore system formed by the hydrocarbon generation during the thermal evolution of kerogen and pyrobitumen in shale. They are the primary reservoir spaces and seepage channels of shale gas. The organic pores can be divided into kerogen pores and pyrobitumen pores depending on the pore genesis.

4.2.2 Development features of organic pores in different thermal maturity stages

According to the previous studies [41], the average organic maturity of the Ordovician-Silurian Wufeng and Longmaxi Formation in Jiaoye-1 well is 2.65%, at the peak of gas generation, and that of Niutitang Formation of Youye-1 well is 3.54%, at the graphitization stage. Compared with Wufeng-Longmaxi Formation located in the

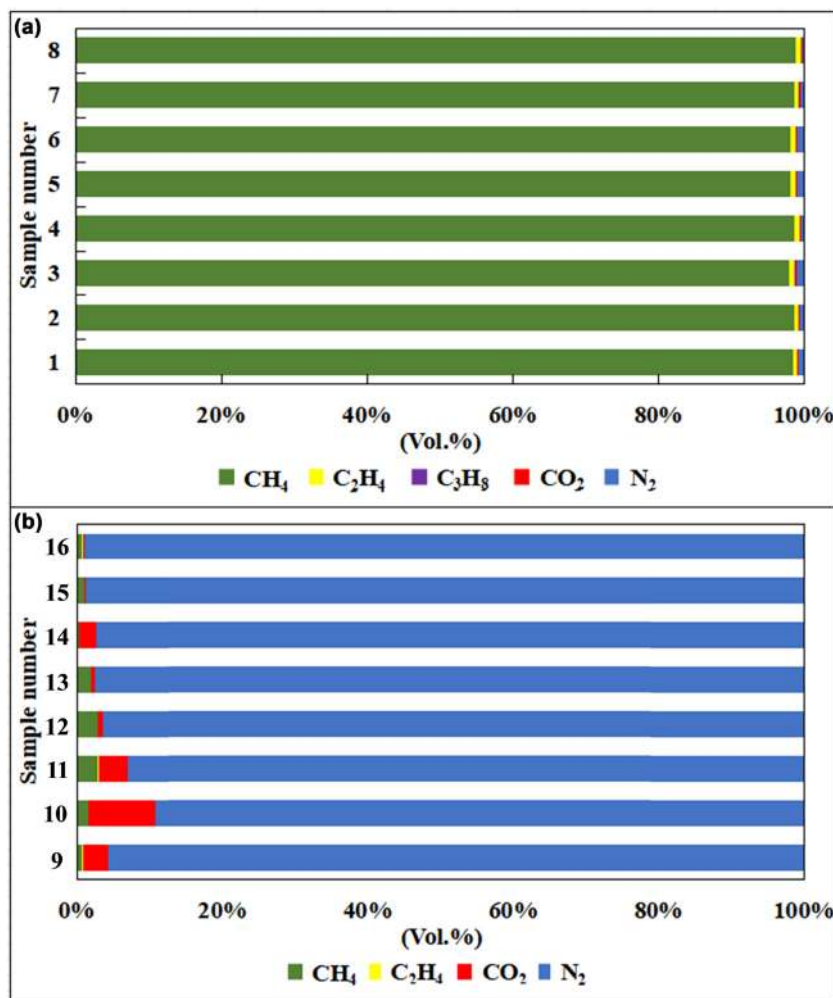


Figure 3: Component analysis of shale gas. (a) Wufeng Formation–Longmaxi Formation section of the Jiaoye-1 well; (b) Niutitang Formation of the Youye-1 well. See Figure 1 for the location of the well site.

upper Ordovician-lower Silurian, Niutitang Formation located in the lower Cambrian experiences more complex structural and thermal evolution and is buried deeper in the geological history. Hence, the maturity of organic matters in the shale of Niutitang Formation is higher than that of Wufeng-Longmaxi Formation [41]. Due to different sedimentation mechanisms, the abundance of organic matter in original sediments of Niutitang Formation is higher than that of Wufeng-Longmaxi Formation, causing the TOC content in the shale of the former is higher than that of the latter [41]. The FIB-SEM experiments were conducted to observe the organic-rich shale images of the two wells. Both Youye-1 well and Jiaoye-1 well have large segments of organic-rich shale. Therefore, the FIB-SEM and FIB-HIM experiments on organic-rich shale are of universality. The shales from the Ordovician-Silurian Wufeng and Longmaxi Formation of the

Jiaoye-1 well mainly develop pyrobitumen pores (Figure 4a), with large pore amount and size and mostly elliptical. The pyrobitumen pores and kerogen pores, in the sample taken from the Niutitang Formation of the Youye-1 well, were not found under 10–100 nm resolution. There are the 1–10 nm pores that cannot be observed under view resolution. Their small pore diameters (Figure 4b) result in poor reservoir capacity when compared with the Jiaoye-1 well.

The FIB-HIM experiment can be used to further observe the internal pore structure. The FIB-HIM was conducted on the samples with the depth near the samples of FIB-SEM. It is observed that there was nesting of small pyrobitumen pores in large pores in the sample taken from the Ordovician-Silurian Wufeng and Longmaxi Formation of the Jiaoye-1 well. Such pore development feature could not only increase the organic

matter reservoir capacity and the specific surface area but also provide the shale gas seepage channels to enhance the connectivity of the organic matter (Figure 5a). Only isolated pores were developed in the organic pores in the sample taken from the Niutitang Formation of Youye-1 well, with a small amount and poor reservoir capacity and poor connectivity (Figure 5b).

4.3 Influencing factors of different maturity levels on shale gas generation and organic pore development

4.3.1 Jiaoye-1 well

Carbon isotope composition is often used to discriminate the generation types of natural gas [42–44]. Figure 6 shows the carbon isotope composition of the shale gas from the Ordovician-Silurian Wufeng and Longmaxi Formation of the Jiaoye-1 well. The $\delta^{13}\text{C}_1$ value is -29.03 to -31.00‰ , with an average value of -30.09‰ . The $\delta^{13}\text{C}_2$ value is -34.60 to -35.90‰ , with an average value of -34.98‰ . There is a significant carbon isotope reversal, i.e. $\delta^{13}\text{C}_1 > \delta^{13}\text{C}_2$.

At present, many studies have been carried out all around the world on the causes of the reversal of shale gas carbon isotope. Most scholars believed that the mixing of different hydrocarbon-generating matrix natural gas (i.e. kerogen cracking gas, liquid hydrocarbon cracking gas) caused the reversal of shale gas carbon isotope [45,46]. Enclosed in the good sealing, when the organic matters evolve to the maturity stage ($R_o = 0.5\text{--}1.2\%$), the liquid hydrocarbons formed by the kerogen will mostly be retained in the inorganic mineral matrix pores (i.e. intragranular pores and intergranular pores) of the organic-rich shale. As the thermal evolution of organic matter continues, when evolving to $R_o = 1.2\text{--}3.5\%$, the liquid hydrocarbon will be bituminized, forming a large number of pyrobitumen pores, as well as the liquid hydrocarbon cracking gas. The kerogen also continues to evolve kerogen pores and form the kerogen cracking gas. According to Zhao [47,48], for $R_o = 1.2\text{--}1.6\%$, the gas generation is mainly due to kerogen cracking, and for $R_o = 1.6\text{--}3.5\%$, it is mainly due to liquid hydrocarbon cracking. The liquid hydrocarbon cracking is about 4 times of kerogen cracking. Since isotope fractionation, ^{12}C is richer than ^{13}C in the liquid hydrocarbon cracking gas and ^{13}C is richer than ^{12}C in the kerogen cracking gas [49–51]. When a large

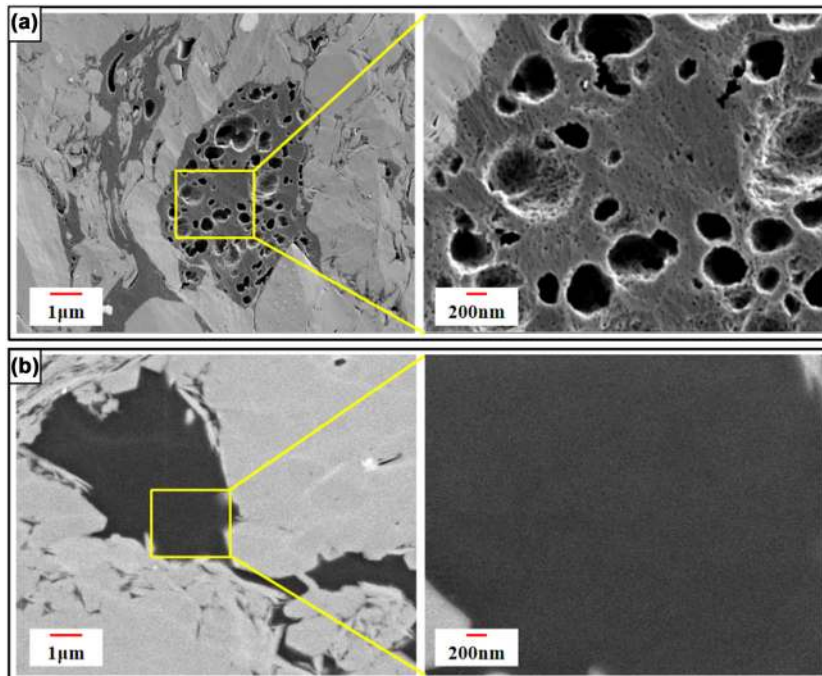


Figure 4: FIB-SEM experimental images. (a) The pyrobitumen pores in the organic-rich shale taken at 2,406 m of Longmaxi Formation section of the Jiaoye-1 well, with large pore amount and size and mostly elliptical; (b) the organic pores in organic-rich shale taken at 3,811 m of Niutitang Formation of the Youye-1 well, with small pore amount and size. See Figure 1 for the well locations.

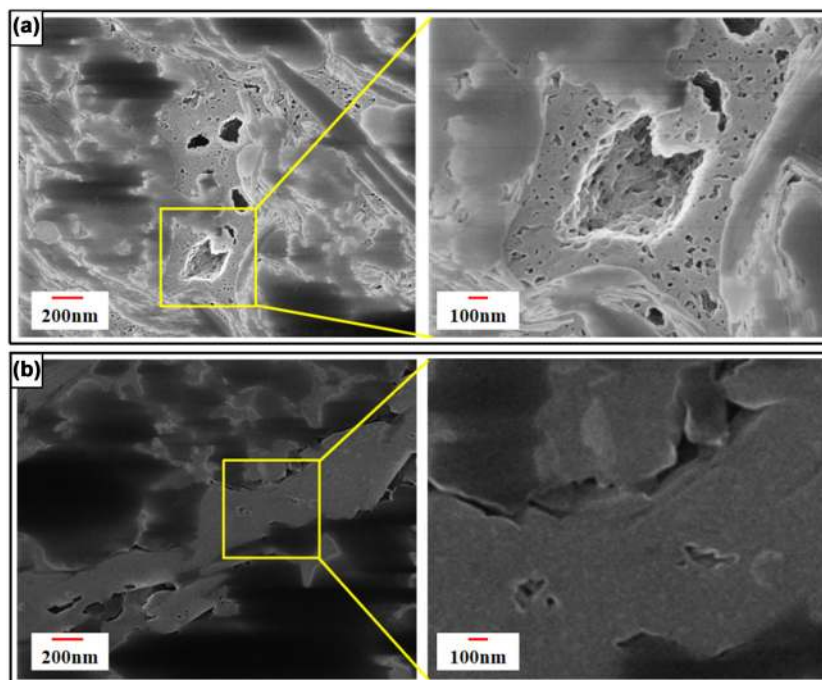


Figure 5: FIB-HIM experimental images. (a) The pyrobitumen pore in the organic-rich shale taken at the 2,404 m Longmaxi Formation of the Jiaoye-1 well has a large number of pores and a large pore diameter. The larger diameter pores are nested in the smaller diameter pores, which can increase the pore reservoir capacity and Connectivity; (b) the organic pores in the organic-rich shale in the 3,813 m Niutitang Formation of the Youye-1 well, with small pore size and inferior pore connectivity. See Figure 1 for the well locations.

amount of liquid hydrocarbon cracking gas is mixed into the kerogen cracking gas, the $\delta^{13}\text{C}_2$ value becomes lower, resulting in the obvious carbon isotope reversal of the shale gas.

The pyrobitumen pores are generated by the bitumization of the liquid hydrocarbon retained in the inorganic mineral matrix pores. The inorganic mineral matrix pores are well resistant to the compaction effect and protect the pyrobitumen pores embedded in it from damage.

Therefore, the pyrobitumen pores are characterized by a large amount, large pore size, strong connectivity and good reservoir capacity. The kerogen pores are formed from the kerogen evolution. The kerogen is deposited simultaneously with inorganic minerals and easily squeezed by inorganic minerals. Under the overlying pressure, the development of the kerogen pores is relatively poor. In such a case, the main reservoir spaces and connecting channels in the shale are pyrobitumen pores.

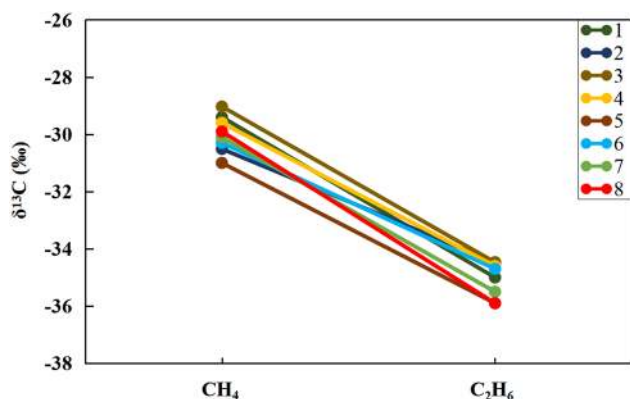


Figure 6: Carbon isotope analysis of shale gas from the lower part of the Longmaxi Formation, Lower Silurian series of Jiaoye-1 well. See Figure 1 for the location of the well site.

4.3.2 Youye-1 well

The major component of the shale gas from the Niutitang Formation of the Youye-1 well is nitrogen, and in contrast, the major component of shale gas from the Ordovician-Silurian Wufeng and Longmaxi Formation of the Jiaoye-1 well is methane and other hydrocarbon gas. The results of nitrogen isotope analysis are shown in Figure 7 with the $\delta^{15}\text{N}$ ranging in $-3\text{‰} \sim +0.5\text{‰}$. Different sources of nitrogen have different origin mechanisms, and their nitrogen isotopic value ranges also vary greatly. According to the previous studies [52–54], the relationship between nitrogen sources, origin mechanisms, and isotope features are summarized in Table 1.

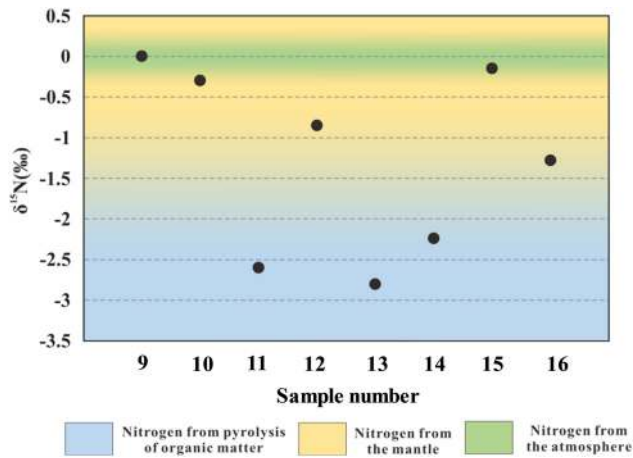


Figure 7: Results of nitrogen isotope analysis of shale gas from Niutitang Formation, lower Cambrian series of the Youye-1 well. See Figure 1 for the location of the well site.

As shown in Figure 7, there are three $\delta^{15}\text{N}$ data points around 0‰, indicating that part of the nitrogen is derived from the atmosphere, and four data points distributed between -10 and -1 ‰, indicating that part of the nitrogen is from the organic matter at the mature-high maturity stage of thermal evolution. There are 5 data points in the range of $-2 \sim +1$ ‰. As mentioned in the previous paragraph, three data points are near 0‰, indicating the presence of atmospheric nitrogen, while one data point is between -10 and -1 ‰, indicating the existence of nitrogen produced by thermal evolution of organic matter in the mature-high maturity stage. When determining the source of nitrogen, it is not only based on the characteristics of the nitrogen isotope but also based on the regional geological background. The volcanic activity has not been found in the history of the Youyang block. Because this data point is close to -10 ‰, near the range indicating the nitrogen from the organic matter at the mature-high maturity stage of thermal evolution, this paper finally attributed the Nitrogen

from the Niutitang Formation of the Youye-1 well to the atmospheric source and thermal evolution at mature-high maturity stage.

The over-mature thermal evolution of the organic matter contributes to the development features of the shale gas origins and organic pores. The organic matter maturity R_o of the Niutitang Formation in the Youye-1 well is of 3.54%, falling into the graphitization stage. With the organic matter evolving to the mature and high maturity stage, the nitrogen due to thermal evolution is generated. Moreover, due to the tectonic compression at the Youyang block, there are several large faults here [55]. The developed faults destroyed the sealing of the shale and its roof and floor, causing the hydrocarbon gas to escape along the faults, as well as the introduction of atmospheric nitrogen. It is the cause of high nitrogen and low hydrocarbons in the shale gas from the Niutitang Formation of the Youye-1 well, and the two nitrogen origins of organic matter thermal evolution and atmosphere.

According to previous studies [56,57], after organic matter (including kerogen and liquid hydrocarbons) evolves to graphitization ($R_o > 3.5\%$), the gas generation potential of shale is close to exhaustion. The adsorption capacity of organic matter to natural gas decreases, and the properties of organic matter change. Under compaction, the organic pores are reduced, resulting in the phenomenon that the number of organic pores developed is small, the pore diameter is small, and the connectivity is poor as shown in Figures 4b and 5b.

5 Pattern summary

After the above experiments and data analysis, the patterns of the thermal evolution of organic matters on shale gas composition, shale gas origins and organic

Table 1: Isotope variation features of different nitrogen sources of shale gas (modified from references [52–54])

Nitrogen source	Origin mechanism	Isotope features
Atmosphere	Deaeration from the surface water entering into the ground	$\delta^{15}\text{N} \approx 0$ ‰
Earth mantle	Nitrogen generated by various thermal and radiation effects inside the earth mantle	$\delta^{15}\text{N} \approx -2$ ‰ \sim $+1$ ‰
Metamorphism	Nitrogen formed by the high temperature metamorphism of nitrogenous minerals	$\delta^{15}\text{N} \approx +1$ ‰ \sim $+3.5$ ‰
Microbial denitrification	Nitrogen generated by the interaction between biomass and organic matters	$\delta^{15}\text{N} \approx -17$ ‰ \sim -10 ‰
Thermal evolution	Nitrogen produced at various evolution stages of organic matters	(immature): $\delta^{15}\text{N} < -10$ ‰ (mature), (high-mature): $\delta^{15}\text{N} \approx -10$ ‰ \sim -1 ‰ (over-mature): $\delta^{15}\text{N} \approx +5$ ‰ \sim $+20$ ‰

pores development can be clarified (Figure 8). The shale organic matters from the lower Cambrian series Niutitang Formation and the Ordovician-Silurian Wufeng and Longmaxi Formation are all type I kerogen. At the maturity level of organic matter $R_o = 0.5\text{--}1.2\%$, the thermal evolution of kerogen produces liquid hydrocarbons, which are mostly retained in the organic-rich shale and filled in the inorganic mineral matrix pores in case of stronger self-sealing of the organic-rich shale and sealing of the shale roof and floor and absent of fault development. The kerogen pores

are formed by the kerogen cracking into liquid hydrocarbon (Figure 8a).

As the increase in depth, the formation temperature also increases. With the maturity level of organic matter reaching $R_o = 1.2\text{--}3.5\%$, kerogen and liquid hydrocarbons produce natural gas. For $R_o = 1.2\text{--}1.6\%$, the kerogen cracking is the dominant process and for $R_o = 1.6\text{--}3.5\%$, the liquid hydrocarbon cracking takes over. The gas generation of liquid hydrocarbon cracking is 4 times that of kerogen cracking in volume. In this organic matter

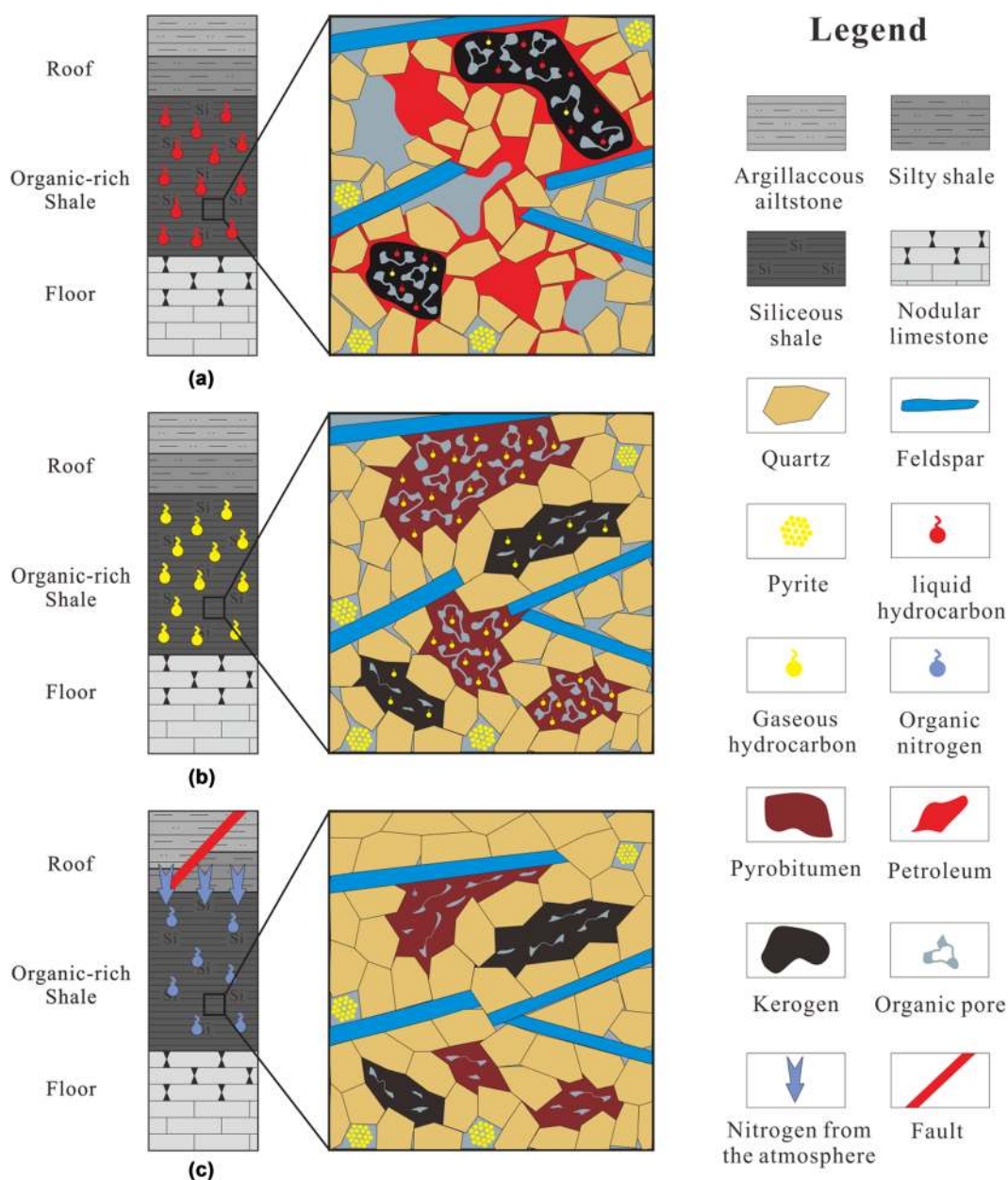


Figure 8: Patterns of thermal evolution of organic matters on shale gas origins and organic pore development. (a) ($R_o = 0.5\%$ to 1.2%), (b) ($R_o = 1.2\%$ to 3.5%), and (c) ($R_o > 3.5\%$).

evolution stage, the shale gas enriched in shale is a blend of kerogen cracking gas and liquid hydrocarbon cracking gas, causing carbon isotope reversal. The liquid hydrocarbon, filling into the pores of the inorganic mineral matrix, is bituminized into liquid hydrocarbon cracking gas while forming a large number of pyrobitumen pores. The inorganic mineral matrix pores are well resistant to the compaction effect and protect the pyrobitumen pores embedded in it from damage, providing the pyrobitumen pores with the features of large amount, large pore size and good connectivity. The kerogen also cracks into natural gas and forming the kerogen pores and easily squeezed by inorganic minerals. As the depth increases, the kerogen pores are squeezed and collapsed under the overlying pressure (Figure 8b).

As the depth continues to increase or under the influence of magmatic activity, the formation temperature reaches a high level. When the maturity of organic matter reaches the stage of graphitization ($R_o > 3.5\%$), the nature of the organic matter changes. Then, the strata begin to uplift, causing faults development, denudation of the overlying strata and the overlying pressure reduced. On the one hand, the hydrocarbon gas escaping and the accumulation of nitrogen from atmospheric sources and the thermal evolution of organic matter results in the composition of high nitrogen and low hydrocarbon. On the other hand, the brittleness of the organic matter changes and under the overlying pressure, the organic pores (pyrobitumen and kerogen pores) collapse, resulting in a less amount of pores, small pore size and poor connectivity (Figure 8c).

6 Conclusions

This article is based on marine organic shale in the Jiaoye-1 well that is located in the southeast of Sichuan basin and Youye-1 well located in the southeast Chongqing of the outer regions of Sichuan basin. The effect of organic maturity on marine shale gas genesis and organic pore development was investigated using a series of experiments such as TOC, gas composition, carbon isotope analysis, nitrogen isotope analysis, FIB-SEM and FIB-HIM. The following are the main conclusions from our study:

(1) When $R_o = 0.5\text{--}1.2\%$, the kerogen generates liquid hydrocarbon by thermal evolution. When stronger self-sealing of the organic-rich shale and sealing of the shale roof and floor and absent of fault development, the liquid hydrocarbon is largely retained in the organic-rich shale and filled into the inorganic

mineral matrix pores. Due to the kerogen cracking into liquid hydrocarbon, kerogen appears in the internal pores.

- (2) When $R_o = 1.2\text{--}3.5\%$, the marine shale gas, which has a high content of methane, is a blend of kerogen cracking gas and liquid hydrocarbon cracking gas, resulting in the reversals of carbon isotope. The organic shale mainly develops pyrobitumen pores with the features of large amount, large pore size and good connectivity.
- (3) When $R_o > 3.5\%$, the organic matter is in the graphitization stage. Complex tectonic movements cause large amounts of shale gas to be lost, resulting in the composition of high nitrogen and low hydrocarbon. Nitrogen comes from the thermal evolution of organic matter and the atmosphere. The organic pores (pyrobitumen and kerogen pores) collapse, resulting in less amount of pores, small pore size and poor connectivity.

Acknowledgments: This study was supported by the China Postdoctoral Science Foundation (No. 2019M663560), the National Natural Science Foundation of China (No. 41872166), the Science and Technology Cooperation Project of the CNPC-SWPU Innovation Alliance, and the Open Fund of Key Laboratory of Tectonics and Petroleum Resources (China University of Geosciences), Ministry of Education, Wuhan (No. TPR-2020-07). We sincerely appreciate all anonymous reviewers and the handling editor for their critical comments and constructive suggestions.

References

- [1] Curtis JB. Fractured shale-gas systems. *AAPG Bull.* 2002;86:1921–38.
- [2] Montgomery SL, Jarvie DM, Bowker KA, Pollastro RM. Mississippian Barnett Shale, Fort Worth basin, north-central Texas: gas-shale play with multi-trillion cubic foot potential. *AAPG Bull.* 2005;89:155–75.
- [3] Zhang K, Peng J, Liu W, Li B, Xia Q, Cheng S, et al. The role of deep geofluids in the enrichment of sedimentary organic matter: a case study of the Late Ordovician-Early Silurian in the upper Yangtze region and early Cambrian in the lower Yangtze region, south China. *Geofluids.* 2020;8868638.
- [4] Horsfield B, Schulz HM. Shale gas exploration and exploitation. *Mar Pet Geol.* 2012;31:1–2.
- [5] Zou C, Yang Z, He D, Wei Y, Li J, Jia A, et al. Theory, technology and prospects of conventional and unconventional natural gas. *Pet Explor Dev.* 2018;45:575–87. (In Chinese with English abstract).

- [6] Ma Y, Cai X, Zhao P. China's shale gas exploration and development: understanding and practice. *Pet Explor Dev.* 2018;45:29–43.
- [7] Nie H, Tang X, Bian R. Controlling factors for shale gas accumulation and prediction of potential development area in shale gas reservoir of South China. *Acta Petrol Sin.* 2009;30:484–91.
- [8] Dong D, Wang Y, Li X, Zou C, Guan Q, Zhang C, et al. Breakthrough and prospect of shale gas exploration and development in China. *Nat Gas Ind.* 2006;36:19–32.
- [9] Zhang K, Jiang Z, Yin L, Gao Z, Wang P, Song Y, et al. Controlling functions of hydrothermal activity to shale gas content-taking lower Cambrian in Xiuwu Basin as an example. *Mar Pet Geol.* 2017;85:177–93.
- [10] Zhang K, Li Z, Jiang S, Jiang Z, Wen M, Jia C, et al. Comparative analysis of the siliceous source and organic matter enrichment mechanism of the Upper Ordovician–Lower Silurian shale in the Upper-Lower Yangtze area. *Minerals.* 2018;8:283.
- [11] Zhang K, Song Y, Jiang S, Jiang Z, Jia C, Huang Y, et al. Mechanism analysis of organic matter enrichment in different sedimentary backgrounds: A case study of the Lower Cambrian and the Upper Ordovician–Lower Silurian, in Yangtze region. *Mar Pet Geol.* 2018;99:488–97.
- [12] Wang P, Jiang Z, Chen L, Yin L, Li Z, Zhang C, et al. Pore structure characterization for the Longmaxi and Niutitang shales in the Upper Yangtze Platform, South China: evidence from focused ion beam-He ion microscopy, nano-computerized tomography and gas adsorption analysis. *Mar Pet Geol.* 2016;77:1323–37.
- [13] Wang P, Jiang Z, Ji W, Zhang C, Yuan Y, Chen L, et al. Heterogeneity of intergranular, intraparticle and organic pores in Longmaxi shale in Sichuan Basin, South China: evidence from SEM digital images and fractal and multifractal geometries. *Mar Pet Geol.* 2016;72:122–38.
- [14] Zou C, Zhu R, Bai B, Yang Z, Wu ST, Su L, et al. First discovery of nano-pore throat in oil and gas reservoir in China and its scientific value. *Acta Petrol Sin.* 2011;27:1857–64 (in Chinese with English abstract).
- [15] Tang X, Jiang Z, Li Z, Gao Z, Bai Y, Zhao S, et al. The effect of the variation in material composition on the heterogeneous pore structure of highmaturity shale of the Silurian Longmaxi Formation in the Southeastern Sichuan Basin, China. *J Nat Gas Sci Eng.* 2015;23:464–73.
- [16] Tang X, Jiang Z, Jiang S, Wang P, Xiang C. Effect of organic matter and maturity on pore size distribution and gas storage capacity in high-mature to post-mature shales. *Energy Fuel.* 2016;30:8985–96.
- [17] Zhang K, Jiang Z, Xie X, Gao Z, Liu T, Yin L, et al. Lateral percolation and its effect on shale gas accumulation on the basis of complex tectonic background. *Geofluids.* 2018;2018:5195469.
- [18] Zhang K, Song Y, Jiang S, Jiang Z, Jia C, Huang Y, et al. Accumulation mechanism of marine shale gas reservoir in anticlines: a case study of the southern Sichuan Basin and Xiuwu Basin in the Yangtze region. *Geofluids.* 2019;2019:5274327.
- [19] Xu Z, Jiang S, Yao G, Liang X, Xiong S. Tectonic and depositional setting of the lower Cambrian and lower Silurian marine shales in the Yangtze Platform, South China: Implications for shale gas exploration and production. *J Asian Earth Sci.* 2019;170:1–19.
- [20] Wałowski G. Experimental assessment of porous material anisotropy and its effect on gas permeability. *Civ Eng J.* 2018;4:906.
- [21] Bahrekazemi S, Hekmatzadeh M. Neuro-simulation tool for enhanced oil recovery screening and reservoir performance prediction. *Emerg Sci J.* 2017;1:54–64.
- [22] Borisova YY, Minzagirova AM, Gilmanova AR, Galikhanov MF, Borisov DN, Yakubov MR. Heavy oil residues: Application as a low-cost filler in polymeric materials. *Civ Eng J.* 2019;5:2554–68.
- [23] Ji W, Song Y, Rui Z, Meng M, Huang H. Pore characterization of isolated organic matter from high matured gas shale reservoir. *Int J Coal Geol.* 2017;174:31–40.
- [24] Ji W, Hao F, Schulz H, Song Y, Tian J. The architecture of organic matter and its pores in highly mature gas shales of the Lower Silurian Longmaxi Formation in the Upper Yangtze Platform, south China. *AAPG Bull.* 2019;102:2909–42.
- [25] Zhang K, Jia C, Song Y, Jiang S, Jiang Z, Wen M, et al. Analysis of Lower Cambrian shale gas composition, source and accumulation pattern in different tectonic backgrounds: A case study of Weiyuan Block in the Upper Yangtze region and Xiuwu Basin in the Lower Yangtze region. *Fuel.* 2020;263:115978.
- [26] Liang X, Zhang T, Yang Y, Zhang Z, Gong Q, Ye X, et al. Microscopic pore structure and its controlling factors of overmature shale in the Lower Cambrian Qiongzhusi Fm., northern Yunnan and Guizhou provinces of China. *Nat Gas Ind.* 2014;32:18–26 (in Chinese with English abstract).
- [27] Wang P, Jiang Z, Han B, Lv P, Jin C, Zhang K, et al. Reservoir geological parameters for efficient exploration and development of Lower Cambrian Niutitang Formation shale gas in South China. *Acta Petrol Sin.* 2018;39(2):152–62.
- [28] Gao Y, Cai X, Zhang P, He G, Gao Q, Wan J. Pore characteristics and evolution of Wufeng–Longmaxi Fms shale gas reservoirs in the basin-margin transition zone of SE Chongqing. *Nat Gas Ind B* 2019;6:323–32.
- [29] Wang X, Shi X, Jiang G, Zhang W. New U–Pb age from the basal Niutitang Formation in South China: implications for diachronous development and condensation of stratigraphic units across the Yangtze platform at the Ediacaran Cambrian transition. *J Asian Earth Sci.* 2012;48:1–8.
- [30] Wu C, Zhang M, Ma W, Liu Y, Xiong D, Sun L, et al. Organic matter characteristic and sedimentary environment of the lower Cambrian Niutitang Shale in Southeastern Chongqing. *Nat Gas Geosci.* 2014;25:1267–74.
- [31] Liu J, Yao Y, Elsworth D, Pan Z, Sun X, Ao W. Sedimentary characteristics of the Lower Cambrian Niutitang shale in the southeast margin of Sichuan Basin, China. *J Nat Gas Sci Eng.* 2016;36:1140–50.
- [32] Dai J, Zou C, Liao S, Dong D, Ni Y, Huang J, et al. Geochemistry of the extremely high thermal maturity longmaxi shale gas, southern sichuan basin. *Org Geochem.* 2014;74:3–12.
- [33] Wang Y, Dong D, Li X, Huang J, Wang S, Wu W. Stratigraphic sequence and sedimentary characteristics of Lower Silurian Longmaxi Formation in the Sichuan Basin and its peripheral areas. *Nat Gas Ind B.* 2015;2:222–32.
- [34] Mou C, Wang X, Wang Q, Zhou K, Liang W, Ge X, et al. Relationship between sedimentary facies and shale gas geological conditions of the Lower Silurian Longmaxi Formation in southern Sichuan Basin and its adjacent areas. *J Palaeogeography.* 2016;18:457–72. (In Chinese with English abstract).

- [35] Li Z, Zhang L, Powell CM. South China in Rodinia: Part of the missing link between Australia-east Antarctica and Laurentia? *Geology*. 1995;23:407–10.
- [36] Li Z, Li X, Zhou H, Kinny PD. Grenvillian continental collision in South China: New SHRIMP U-Pb zircon results and implications for the configuration of Rodinia. *Geology*. 2002;30:163–6.
- [37] Wang J, Li Z. History of Neoproterozoic rift basins in South China: Implications for Rodinia break-up. *PreCambrian Res*. 2003;122:141–58.
- [38] Wei X, Guo T, Liu R. Geochemical features and genesis of shale gas in the Jiaoshiba Block of Fuling Shale Gas Field, Chongqing, China. *J Nat Gas Geosci*. 2016;27:539–48.
- [39] Yang R, He S, Hu Q, Hu D, Yi J. Geochemical characteristics and origin of natural gas from Wufeng-Longmaxi shales of the Fuling gas field, Sichuan Basin (China). *Int J Coal Geol*. 2017;171:1–11.
- [40] Jiao W, Wang S, Cheng L, Luo Q, Fang G. The reason of high nitrogen content and low hydrocarbon content of shale gas from the Lower Cambrian Niutitang Formation in southeast Chongqing. *Nat Gas Geosci*. 2017;28:1882–90 (in Chinese with English abstract).
- [41] Zhao W, Li J, Yang T, Wang S, Huang J. Geological difference and its significance of marine shale gases in South China. *Pet Explorat Dev*. 2016;43:499–510 (in Chinese with English abstract).
- [42] Schoell M. Genetic characterization of natural gases. *AAPG Bull*. 1983;67:2225–38.
- [43] Dai J. Significance of the study on carbon isotopes of alkane gases. *Nat Gas Ind*. 2011;31:1–6. (In Chinese with English abstract).
- [44] Dai J, Ni Y, Gong D, Feng Z, Liu D, Peng W, et al. Geochemical characteristics of gases from the largest tight sand gas field (Sulige) and shale gas field (Fuling) in China. *Mar Pet Geol*. 2019;79:426–38.
- [45] Tilley S, McLellan S, Hiebert B, Quatero B, Veilleux K. Muehlenbachs, gas isotopic reversals in fractured gas reservoirs of the western Canadian Foothills: mature shale gases in disguise. *AAPG Bull*. 2011;95:1399–422.
- [46] Hao F, Zou H. Cause of shale gas geochemical anomalies and mechanisms for gas enrichment and depletion in high-maturity shales. *Mar Pet Geol*. 2013;44:1–12.
- [47] Zhao W, Wang Z, Zhang S, Wang H, Zhao C, Hu G. Successive generation of natural gas from organic materials and its significance in future exploration. *Pet Explorat Dev*. 2005;32:1–7.
- [48] Zhao W, Wang Z, Wang H, Li Y, Hu G, Zhao C. Further discussion Oil the connotation and significance of the natural gas relaying generation model from organic materials. *Pet Explorat Dev*. 2011;38:129–35.
- [49] James AT. Correlation of natural gas by use of carbon isotopic distribution between hydrocarbon components. *AAPG Bull*. 1983;67:1176–91.
- [50] Rooney MA, Claypool GE, Chung HC. Modeling thermogenic gas generation using isotope ratios of natural gas hydrocarbons. *Chem Geol*. 1995;126:219–32.
- [51] Tang Y, Perry JK, Jenden PD, Schoell M. Mathematical modeling of stable carbon isotope ratios in natural gases. *Geochim Cosmochim Acta*. 2000;64:2673–87.
- [52] Zeng Z. Genetic type of nitrogen gas in sedimentary basins in China. *Nat Gas Geosci*. 2002;13:29–33.
- [53] Liu Q, Liu W, Kross BM, Wang W, Dai J. Advances in nitrogen geochemistry of natural gas. *Nat Gas Geosci*. 2006;17:119–24.
- [54] Krooss BM, Littke R, Müller B, Frielingsdorf J, Schwochau K, Idiz EF. Generation of nitrogen and methane from sedimentary organic matter: Implications on the dynamic of natural gas accumulations. *Chem Geol*. 1995;126:291–318.
- [55] Zeng W, Zhang J, Ding W, Zhao S, Zhang Y, Liu Z, et al. Fracture development in Paleozoic shale of Chongqing area (South China). Part one: fracture characteristics and comparative analysis of main controlling factors. *J Asian Earth Sci*. 2013;75:251–66.
- [56] Ji C, Xiao X. Evolution of nanoporosity in organic-rich shales during thermal maturation. *Fuel*. 2014;129:173–81.
- [57] Wang Y, Dong D, Cheng X, Huang J, Wang S, Wang S. Electric property evidences of the carbonification of organic matters in marine shales and its geologic significance: a case study of the Lower Cambrian Qiongzhusi Shale in the southern Sichuan Basin. *Nat Gas Ind*. 2014;34:1–7.